Fatty Acid Modulated Human Serum Albumin Binding of the β-Carboline Alkaloids Norharmane and Harmane

ARTICLE *in* MOLECULAR PHARMACEUTICS · OCTOBER 2013

Impact Factor: 4.38 · DOI: 10.1021/mp400531n · Source: PubMed

molecular pharmaceutics

Article

pubs.acs.org/molecularpharmaceutics

Fatty Acid Modulated Human Serum Albumin Binding of the β-Carboline Alkaloids Norharmane and Harmane

Celesztina Domonkos, Ilona Fitos, Júlia Visy, and Ferenc Zsila*

Department of Biochemical Pharmacology, Institute of Molecular Pharmacology, Research Centre for Natural Sciences, Hungarian Academy of Sciences, POB 17, H-1025, Budapest, Hungary

Supporting Information

ABSTRACT: Harmane and norharmane are representative members of the large group of natural β-carboline alkaloids featured with diverse pharmacological activities. In blood, these agents are transported by human serum albumin (HSA) which has a profound impact on the pharmacokinetic and pharmacodynamic properties of many therapeutic drugs and xenobiotics. By combination of various spectroscopic methods, the present contribution is aimed to elucidate how nonesterified fatty acids (FAs), the primary endogenous ligands of HSA, affect the binding properties of harmane and norharmane. Analysis of induced circular dichroism (CD) and fluorescence spectroscopic data indicates the inclusion of the neutral form of both molecules into the binding pocket of subdomain IIIA, which hosts two FA binding sites, too. The induced CD and UV absorption spectra of harmane and norharmane exhibit peculiar changes upon addition of FAs, suggesting the formation of ternary complexes in which the lipid ligands significantly alter the binding mode of the alkaloids via cooperative allosteric mechanism. To our knowledge, it is the first instance of the demonstration of drug-FA cobinding at site IIIA. In line with these results, molecular docking calculations showed two distinct binding positions of norharmane within subdomain IIIA. The profound increase in the affinity constants of β-carbolines estimated in the presence of FAs predicts that the unbound, pharmacologically active serum fraction of these compounds strongly depends on the actual lipid binding profile of HSA.

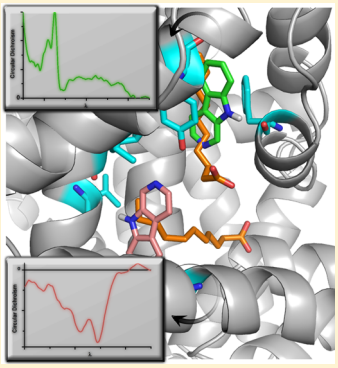

KEYWORDS: *allosteric interaction, β-carbolines, circular dichroism, fatty acid, harmane, human serum albumin, norharmane*

INTRODUCTION

The β-carboline alkaloids are a large group of natural indole alkaloids that possess a common tricyclic pyrido[3,4]indole ring structure. They are present in numerous plants including *Peganum harmala* and *Passiflora incarnata* which have been traditionally used for hundreds of years to treat gastrointestinal diseases and malaria.[1] The occurrence of β-carboline alkaloids in commonly ingested foodstuffs refers to that diet is an important exogenous source of these compounds in humans.[2] However, the endogenous origin of harmane (1-methyl-9*H*-pyrido-[3,4-*b*]indole) and norharmane (9*H*-pyrido[3,4-*b*]-indole) was also demonstrated in various tissues and physiological fluids, where they can be formed by cyclization of tryptamine.[3,4] Some reports indicated that the levels of β-carbolines in plasma and cerebrospinal fluid may augment in certain disorders and they may play a role in the pathogenesis of Parkinson's disease. Furthermore, several lines of evidence have already shown that these substances also exhibit significant antioxidant abilities and neuroprotective effects against neurotoxins.[5] Besides their impact on the central nervous system, recent research has been focused on the potent antitumor, antiviral, antimicrobial, and antiparasitic activities of these agents as well as their application in photodynamic therapy.[1]

Human serum albumin (HSA) is the most abundant protein in the circulatory system (~0.6 mM) which accounts for 60−65% of the total plasma protein concentration.[6] The 66.5 kDa single polypeptide chain of HSA consists of 585 amino acids and is folded into three homologous domains (I, II, and III), each of which consisting two subdomains ("A" and "B"). The enormous ligand binding capability of HSA renders it the most important cargo of blood plasma affecting the pharmacokinetics of numerous therapeutic drugs and other bioactive agents.[7,8] In many instances, HSA binding affinity chiefly impacts the free plasma fraction of drugs which is responsible for the pharmacological action; thus the study of drug−HSA interactions is an essential task in determining therapeutic doses. Three preformed, flexible hydrophobic cavities located within the subdomain IB, IIA, and IIIA represent the principal binding regions of HSA (site IB, IIA, and IIIA) where chemically diverse, exo- and endogenous compounds can be bound.[9,10] Typically, the high-affinity ligands of these sites are anionic or neutral in nature such as hemin, biliverdin, camptothecin, and teniposide for site IB,[10,11] warfarin, azapropazone, phenylbutazone, and iodipamide for site IIA,[9] and ibuprofen, diflunisal, iophenoxic acid, and diazepam for site IIIA.[9,12]

Received: September 2, 2013
Revised: October 29, 2013
Accepted: October 30, 2013
Published: October 30, 2013

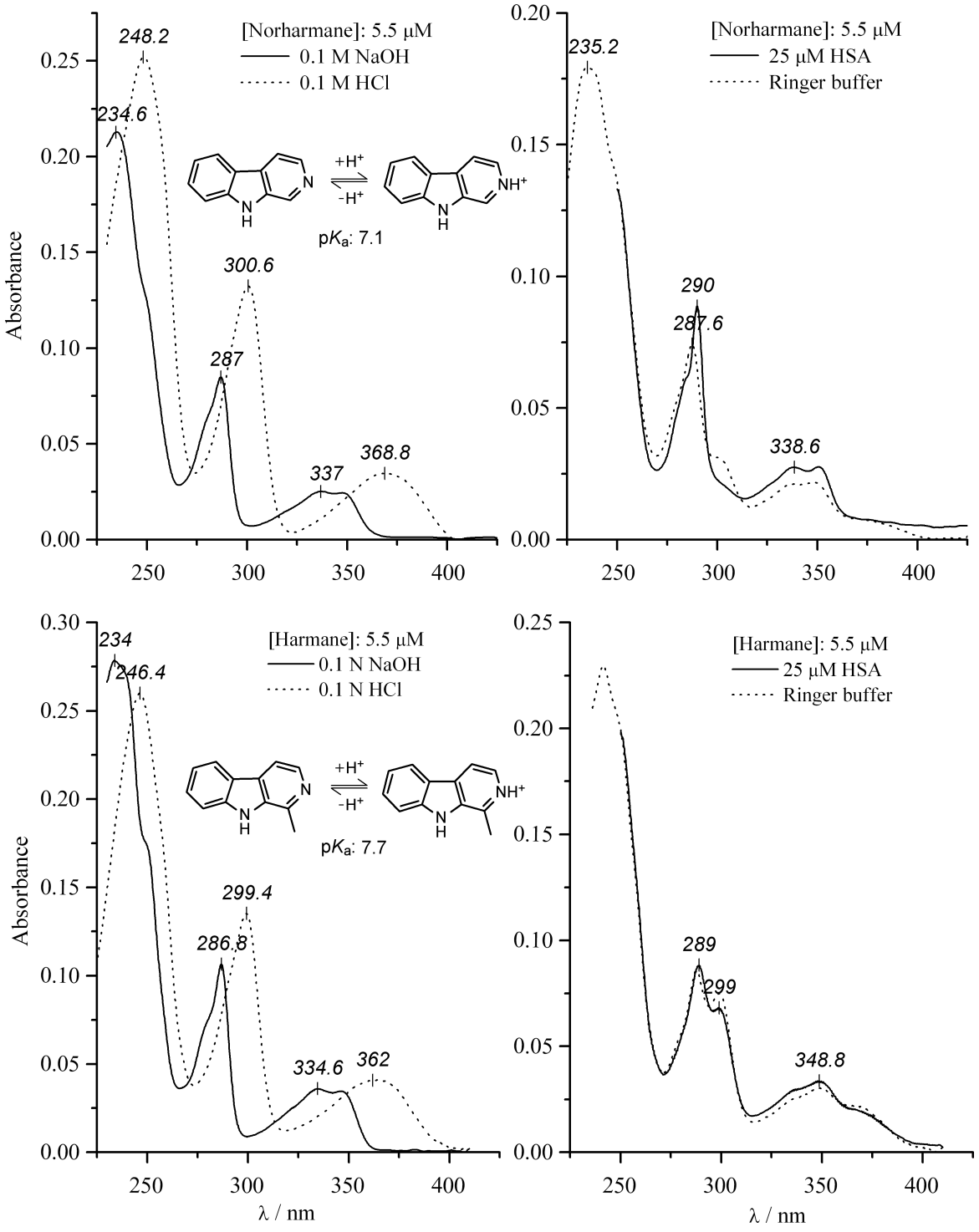

Figure 1. UV absorption spectra of norharmane and harmane measured in basic and acidic solutions and at physiological pH in the presence and absence of HSA. Acid−base equilibrium and pK_a values of the alkaloids are shown.

In relation to acidic and neutral drugs, less attention has been devoted for the HSA binding of basic compounds though the tight HSA association of Vinca alkaloids has been demonstrated.[13] HSA binding of some β-carbolines has already been studied, but the results are contradictory both in the context of the affinity constant as well as the binding location of these compounds.[14−16] Therefore, the main aim of this work is to assess the HSA binding interactions of two representative β-carboline alkaloids, harmane and norharmane, by using various spectroscopic methods complemented with molecular docking calculations. Since the nonesterified fatty acids (FAs) are the primary endogenous ligands of serum albumin,[17] their effect on the HSA association of β-carbolines is also elucidated.

MATERIALS AND METHODS

Materials. HSA (Sigma, A1887, 97%, essentially fatty acid-free), norharmane HCl (Sigma), harmane (Servier Research Institute of Medicinal Chemistry, Budapest, Hungary),

dx.doi.org/10.1021/mp400531n | Mol. Pharmaceutics 2013, 10, 4706−4716

biliverdine HCl (Frontier Scientific), hemin (Frontier Scientific), myristic acid (Sigma), palmitic acid (Sigma), oleic acid (Fluka), (±)-carprofen (S.C. VIM SPECTRUM S.R.L., Romania), (±)-naproxen (AK Scientific, Inc.), (*S*)-ibuprofen (Research Biochemicals International), and propofol (Sigma) were used as supplied.

Preparation of Ligand and Protein Sample Solutions. The 2 mM stock solutions of β-carbolines were prepared freshly before each measurement in ultrapure water (norharmane HCl) or in the 1:1 (v/v) mixture of ethanol/water or in dimethyl sulfoxide (DMSO; harmane). Water, water−DMSO, and buffer−DMSO mixtures were used to dissolve other compounds. The volume of DMSO added into sample solutions never exceeded 5% (v/v) and caused negligible effects either on the CD or the fluorescence spectra. HSA samples were dissolved in pH 7.4 Ringer buffer solution (8.1 mM $Na_2HPO_4{\cdot}12H_2O$, 1.5 mM KH_2PO_4, 137 mM NaCl, 2.7 mM KCl, 0.8 mM $CaCl_2$, 1.1 mM $MgCl_2$).

Circular Dichroism and UV Absorption Spectroscopy Measurements. CD and UV absorption spectra were recorded on a JASCO J-715 spectropolarimeter at 25 ± 0.2 °C. Temperature control was provided by a Peltier thermostat equipped with magnetic stirring. Rectangular quartz cells of a 1 cm optical path length (Hellma, USA) were used. Each spectrum represents the average of three scans obtained by collecting data at a scan speed of 100 nm/min. Absorption spectra were obtained by conversion of the high voltage (HT) values of the photomultiplier tube of the CD equipment into absorbance units. CD and absorption curves of ligand−HSA mixtures were corrected by subtracting the spectra of ligand-free HSA solution. JASCO CD spectropolarimeters record CD data as ellipticity (θ) in units of millidegrees (mdeg).

Calculation of HSA Binding Parameters of Norharmane. Details of the estimation of the association constant (K_a) and the number of binding sites (n) using CD spectroscopic data have been described elsewhere.[18] Nonlinear regression analysis of the induced CD values measured at different [ligand]/[HSA] molar ratios was performed by Microcal Origin 8.6 Pro (OriginLab Corporation, Northhampton, MA).

Fluorescence Spectroscopic Measurements. Fluorescence measurements were carried out in a Jasco FP 8300 spectrofluorimeter at 23 ± 1 °C, using a quartz cuvette with 1 cm optical path length; both bandwidths were 5 nm. The β-carbolines were excited at 320 nm. Quenching of intrinsic HSA fluorescence was measured at 280 nm/330 nm. Intensities were corrected for the inner filter effects according to the absorbance of the added alkaloids at both the excitation and the emission wavelengths. The association binding contants were calculated by the following equation assuming 1:1 stoichiometry, using nonlinear regression analysis (Microcal Origin ver. 8.6):

$$F = ([P]_t - [L]_t - [K]_D) \times \frac{f_p}{2} + ([L]_t - [P]_t - [K]_D) \times \frac{f_l}{2} + ([P]_t + [L]_t + [K]_D) \times \frac{f_{pl}}{2} + (f_p + f_l - f_{pl}) \times \sqrt{\frac{([P]_t + [L]_t + [K]_D)^2}{4} - [P]_t \times [L]_t}$$

where $[P]_t$ and $[L]_t$ are the total concentrations of the protein and ligand; f_p, f_l, f_{pl} are the specific fluorescence of the protein, ligand, and complex.[19]

Molecular Docking Calculations. Docking calculations were carried out using the DockingServer.[20] The PM6 semiempirical method (MOPAC2009) was used for energy minimization and partial charges calculation to harmane and norharmane. The X-ray structure of HSA complexed with myristic acid (PDB code 1BJ5) was selected. All water molecules were removed from the protein coordinates prior to docking calculations. Hydrogen atoms were added to the PDB structure using AutoDockTools. The total charge of HSA and partial charges of the atoms were calculated by the Mozyme function of MOPAC2009 software. The calculated partial charges were applied for further calculations. Affinity (grid) maps of 25 × 25 × 25 Å grid points were generated using the Autogrid program. AutoDock parameter set- and distance-dependent dielectric functions were used in the calculation of the van der Waals and the electrostatic terms, respectively. Docking simulations were performed using the Lamarckian genetic algorithm and the Solis and Wets local search method. The initial position and orientation of deprotonated forms of harmane and norharmane were set randomly. Each docking experiment was derived from 100 different runs that were set to terminate after a maximum of 2 500 000 energy evaluations. The population size was set to 150. During the search, a translational step of 0.2 Å and quaternions and torsion steps of 5 were applied. The outputs of docking calculations were rendered with PyMOL (The PyMOL Molecular Graphics System, DeLano Scientific LLC, Palo Alto, CA, USA; http://www.pymol.org).

RESULTS

Effect of pH and HSA Binding on the UV Absorption Spectrum of β-Carbolines. The pK_a of the pyridine nitrogen of norharmane (≈7.1) is close to the physiological pH value, while the corresponding value of the pyrrole ring is higher by several orders of magnitude (≈11).[21,22] Thus, the molecule exhibits remarkable light absorbance changes in a pH-dependent fashion.[21,22] The UV spectrum of norharmane recorded in acidic solution is determined by the protonated form, but under alkaline conditions the neutral species is predominant (Figure 1). Transformation from the neutral to the cationic form results in strong hyperchromism and bathochromic shifts of the UV peaks. At pH 7.4, above the pK_a value of norharmane, both forms are present with the relative dominance of the neutral species which is reflected in the absorption spectrum measured in Ringer buffer solution (Figure 1). Upon addition of norharmane to the aqueous buffer solution of HSA, the shoulder around 300 nm which is characteristic to the cationic species vanishes, and the UV maximum measured at 287 nm in protein-free buffer solution shows a 3 nm red shift (Figure 1). It suggests that the HSA binding shifts the cationic-neutral equilibrium toward the nonprotonated form of norharmane. In relation to norharmane, UV contribution of the protonated form of harmane is more prevalent at physiological pH due to its higher pK_a, as it is suggested by the broadened bands and the much larger intensity of the 300 nm peak. In water the pK_a of 7.7 was measured,[21] but due to the high ionic strength of the Ringer buffer this value may be lower. HSA binding only slightly modifies the absorption spectrum in favor of the neutral form (Figure 1), suggesting either weak binding or only weak preference of the neutral species in the presence of protein.

CD Spectroscopic Investigation of the HSA Binding. HSA association of harmane induces no difference CD signals.

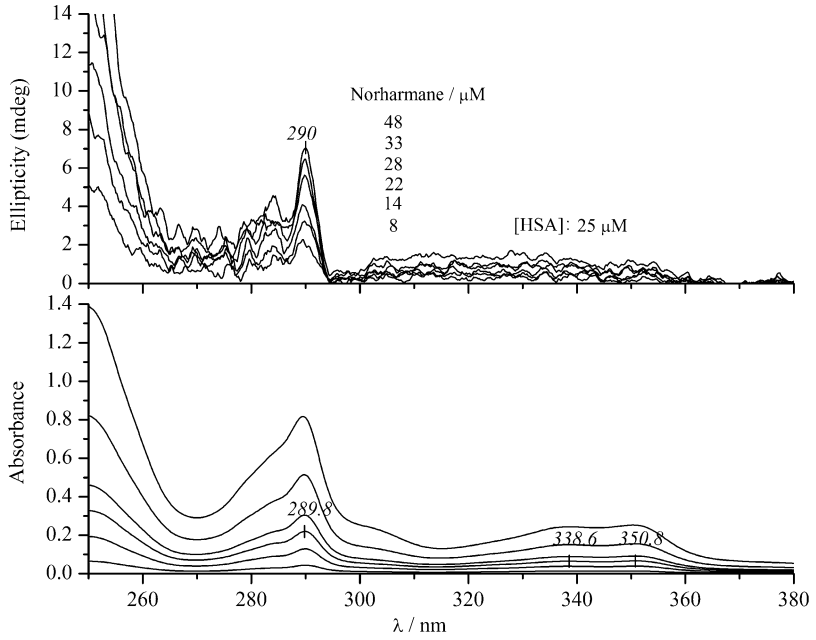

Figure 2. Difference CD and UV absorption spectra of norharmane measured in HSA solution at increasing ligand/protein molar ratios (Ringer buffer, 25 °C).

In contrast to this, titration of HSA with small aliquots of norharmane stock solution results in three positive ellipticity bands allied to the UV absorption peaks of the ligand (Figure 2). Both the shape and the relative intensity of these signals are similar to the corresponding absorption bands. Unfortunately, the most intense, short-wavelength induced CD (ICD) peak is only partially resolved due to the strong interference of the intrinsic CD contribution of HSA. To estimate the binding affinity of norharmane, CD values were recorded at 290 nm by adding the alkaloid to HSA solution (25 μM). Nonlinear regression analysis of the data plotted against the total ligand concentration of the sample indicated strong binding of norharmane to a single site of HSA (Supporting Information, Figure 1). The K_a value obtained by this way (1.8×10^5 M^{-1}) is in a good agreement with previous fluorescence spectroscopic measurements.[14] However, conflicting data are available on the HSA binding location of β-carbolines predicting domain I[14] and subdomain IIIA[15] for norharmane, as well as subdomain IIA for harmane.[16]

Mapping HSA Binding Site of Norharmane. CD displacement experiments were performed using specific CD labels of the principal drug binding regions of HSA. In the presence of competing agents having the same binding area, the ICD signal of the HSA bound site marker ligand decreases. Biliverdin was chosen as the selective CD marker of site IB.[10] The changes of the ICD signal of the bound label were monitored in the presence of increasing concentrations of norharmane. There is negligible overlap between the induced ellipticity peak of biliverdin at 385 nm and the longest wavelength ICD band of norharmane. If biliverdin and norharmane shared a common binding room, its addition should cancel the ICD band of the pigment. Instead of reduction, however, stepwise addition of the alkaloid gradually enhanced the ICD amplitude of biliverdin (Supporting Information, Figure 2). To fully exclude the site IB binding of norharmane, an additional titration was conducted using the hemin bound form of HSA. The hemin–HSA binding interaction is extremely strong ($K_a \sim 10^8$ M^{-1}), and the large macrocycle completely occupies the binding cavity of subdomain IB.[11] Therefore, in the presence of hemin other ligand molecules could not be bound here. However, addition of norharmane to the equimolar mixture of hemin:HSA resulted in the same ICD pattern which was previously measured with hemin-free HSA samples (data not shown, ICD contribution of HSA bound hemin was subtracted).

Unfortunately, the ICD signals of norharmane and conventional site IIA (azapropazone,[23] phenylbutazone[24]) and site IIIA (diazepam[24]) markers are displayed in the same spectral regions which precludes to derive reliable conclusions from CD displacement experiments. However, there are some site IIIA ligands including ibuprofen ($K_a \sim 10^6$ M^{-1}), naproxen ($K_a \sim 10^6$ M^{-1}), and propofol ($K_a \sim 10^5$ M^{-1}), the HSA complexes of which show no detectable ICD activity above 260 nm; thus they can be used to probe the binding site of norharmane (the very weak intrinsic CD signals of (*S*)-ibuprofen above 250 nm were negligible under the experimental settings applied). (*S*)-ibuprofen and (±)-naproxen reduced to zero the 290 nm ellipticity peak of norharmane around the 1:1 drug–HSA molar ratio (Figure 3), while propofol even in high excess (6:1) decreased the CD amplitude by half only. Distinctly from naproxen and propofol of which UV bands above 250 nm overlap with the absorption peaks of norharmane, the UV contribution of the unconjugated phenyl ring of ibuprofen is negligible in that region. The increase of ibuprofen concentration in the sample solution resulted in a small blue shift and intensity loss of the main UV peak of norharmane. In parallel with this, a shoulder developed above 295 nm which is similar to that measured in protein-free buffer solution (spectra not shown).

The primary, high-affinity ($K_a \sim 10^6$ M^{-1}) HSA binding site of the antiinflammatory drug carprofen corresponds to the indole–benzodiazepine area in subdomain IIIA.[25] Since the aromatic moiety of carprofen is very similar to that of norharmane, it is reasonable to assume that they share a common binding region. The HSA association of (±)-carprofen also induces multiple, positive ICD bands between 250 and

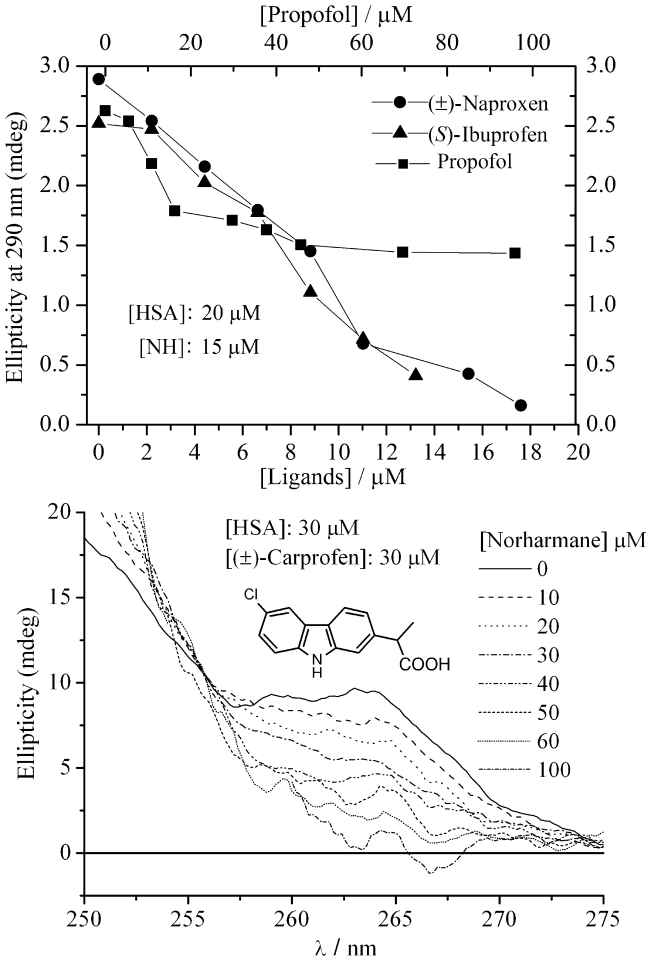

Figure 3. Top panel: Changes of the ICD values of HSA bound norharmane upon stepwise addition of the site IIIA marker ligands (±)-naproxen, (*S*)-ibuprofen, and propofol (Ringer buffer, 25 °C). Bottom panel: Effect of addition of norharmane on the ICD spectrum of HSA bound (±)-carprofen (Ringer buffer, 25 °C).

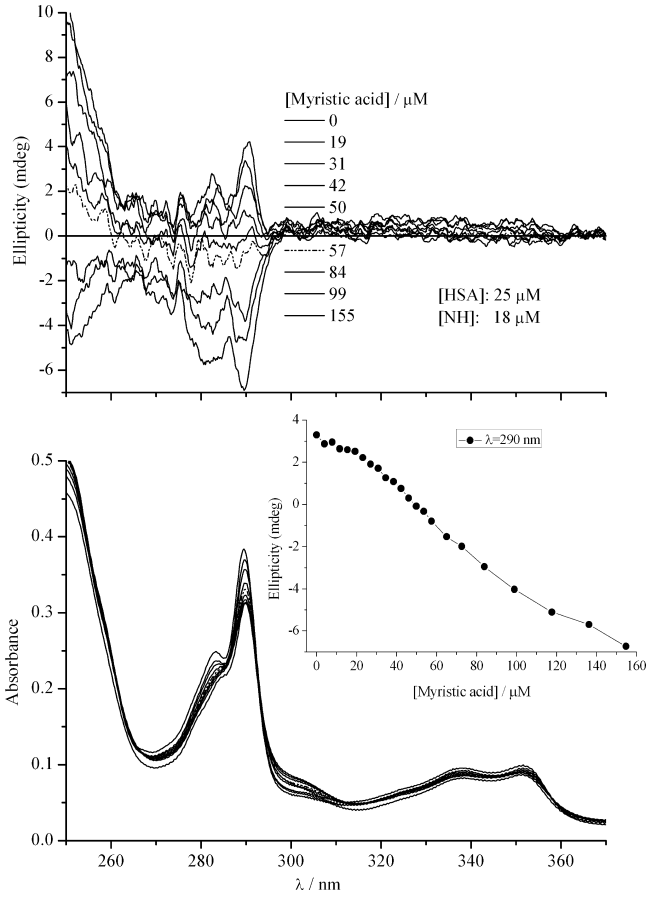

Figure 4. CD and absorption spectral changes measured upon stepwise addition of myristic acid into the mixture of norharmane and HSA (Ringer buffer, 25 °C). Inset: Induced ellipticity values measured at 290 nm plotted against the myristic acid concentration of the sample solution.

360 nm,[25] two of which display complete overlap with the bands of norharmane (Figure 3). Fortunately, in the region of the partially resolved peak of carprofen around 262 nm, the ICD values of norharmane are six times weaker which enables to conduct CD competition measurements. The addition of norharmane into the carprofen-HSA mixture progressively decreased this ellipticity band to zero (Figure 3).

CD Spectroscopic Study of the Effects of Saturated and Unsaturated Dietary Fatty Acids on the HSA Binding of *β*-Carbolines. The crystallographically verified seven common binding sites of medium/long-chain saturated and unsaturated FAs (sites 1−7) are asymmetrically distributed across the domains of HSA.[17,26,27] Occupation of the high-affinity FA sites (2 in IA/IIA, 4 in IIIA, and 5 in IIIB) induces local as well as global conformational changes of the protein which frequently affect the ligand binding properties of HSA.[17] FAs can displace bound agents via direct binding competition, or they can enhance or reduce the HSA affinity of drugs by allosteric mechanisms.[28,29] The lower-affinity FA sites 1 (IB), 3 (IIIA), and 7 (IIA) overlap with the three principal drug binding regions of HSA.[27]

On stepwise addition of myristic acid to HSA−norharmane solution, the induced ellipticity values declined slowly (Figure 4). Above the 1:1 FA−HSA molar ratio, the intensity loss accelerated, and the ICD signal was reduced to zero around a 2:1 ratio. Upon further FA addition, a mirror-image like ICD pattern evolved together with considerable alterations of the UV spectrum including hyperchromism of the 290 nm peak and vanishing of the shoulder at about 300 nm. To elucidate how FA binding affects the association constant of norharmane, further CD titrations were performed by using fatted HSA samples prepared by addition of myristic acid into the HSA sample solution to achieve 1:1, 3:1, and 4:1 FA−protein molar ratios. Subsequently, these samples were titrated with norharmane, and the affinity constants were calculated from the ICD data. At 1:1 and 3:1 molar ratios the K_a values do not differ significantly from the constant obtained with defatted HSA sample. At a 4:1 ratio, however, the estimated affinity constant is three times higher, attesting tighter alkaloid−HSA binding interaction. The use of palmitic and oleic acid resulted in very similar CD and absorption spectroscopic changes (not shown), and the association constant was even higher (Table 1). It is to be noted that, distinctly from C14 and C16 FAs, the maximum affinity enhancement was achieved with three mole equivalents of the unsaturated oleic acid (C18).

In contrast to the FA-free state, CD titration of palmitic acid-HSA complexes with harmane showed the development of a negative ICD signal around 290 nm (Figure 5), which is similar to that measured with norharmane under identical experimental conditions. It can be also observed that the addition of palmitic

Table 1. HSA Association Constants of Harmane and Norharmane Estimated from CD and Fluorescence Data in the Absence and Presence of Nonesterified FAs[a]

	K_a (M^{-1})	f_b (%)	fatty acid	[FA] (μM)	[HSA] (μM)	method
harmane	2.4 (±0.1) × 10^4	93.5				fluoresc.
	1.5 (±0.2) × 10^5	98.9	myristic acid	80	20	fluoresc.
	1.2 (±0.1) × 10^5	98.6	palmitic acid	80	20	fluoresc.
	2.4 (±0.4) × 10^5	99.3	oleic acid	40	20	fluoresc.
norharmane	1.7 (±0.1) × 10^5	99.0				fluoresc.
	1.8 (±0.3) × 10^5	99.1			25	CD
	2.6 (±0.4) × 10^5	99.4	myristic acid	80	20	CD
	4.5 (±0.7) × 10^5	99.6	palmitic acid	80	20	CD
	3.7 (±0.6) × 10^5	99.5	oleic acid	60	20	fluoresc.

[a]HSA bound fraction (f_b) of the alkaloids approximated from the K_a values are shown. The formula applied to estimate f_b values: $f_b = (K_a \times [HSA])/(K_a \times [HSA] + 1)$ where [HSA] is 600 μM and [ligand] ≪ [HSA].

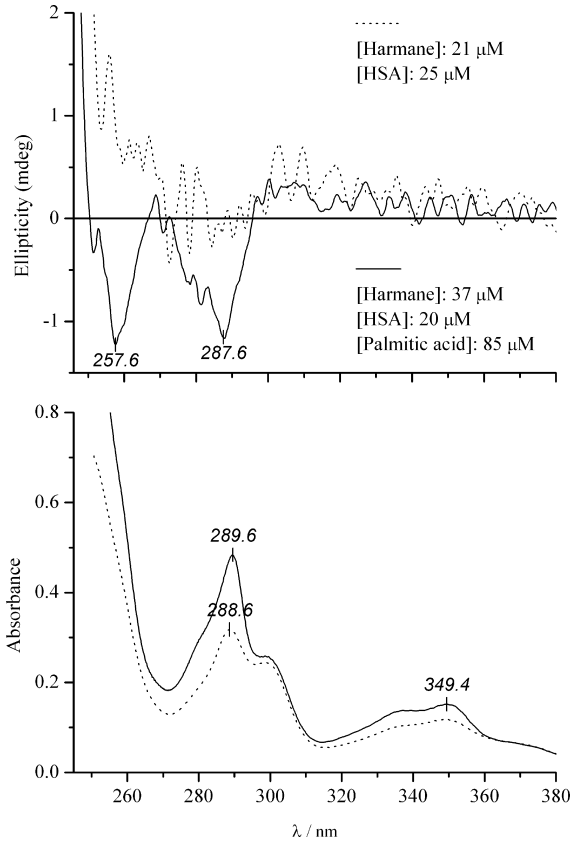

Figure 5. Effect of palmitic acid on the CD and UV absorption spectra of HSA bound harmane (Ringer buffer, 25 °C).

acid into the harmane–HSA mixture considerably perturbs the absorption bands of the ligand, too (Figure 5). The intensity ratio of the 290 nm peak and the shoulder around 300 nm significantly increases, indicating enhanced contribution of the neutral form (cf. Figure 1). The applied different harmane concentrations are not supposed to provoke considerable changes.

Fluorescence Spectroscopic Investigation of Harmane–HSA Interaction in the Absence and Presence of Fatty Acids. The fluorescence method has successfully been applied to study the binding of norharmane to HSA.[14] The ligand solution at pH 7.0 showed a single, unstructured band at 450 nm ascribed to the cationic species. By gradual addition of HSA, a peak at 380 nm appeared at the cost of the cationic form, ascribed to the neutral species. This low quantum yield emission signal was used to calculate the association binding constant (K_a = 1.25 × 10^5 M^{-1}).[14] We performed analogous fluorescence measurements, resulting in a K_a value of 1.7 × 10^5 M^{-1}.

It is to be noted that the dominance of the cationic emission peak of β-carbolines in buffer solution around pH 7.0 is not in accordance with the absorbance spectra. This phenomenon can be interpreted with the excited state pK_a shift (~13) of these compounds.[22] The HSA binding seems to stabilize the neutral form.

A similar study was conducted with harmane, as well. In buffer solution it exhibits an emission peak at 434 nm (Figure 6). By the gradual addition of HSA, the intensity of this peak decreases, with simultaneous development of a structured band with two maxima resolved at 361 and 378 nm, representing the bound, neutral form of harmane. Based on the increasing emission intensities, a K_a value of 2.4 × 10^4 M^{-1} could be calculated (Table 1).

CD measurements proved that fatty acids have profound impact on both the strength and the mode of the albumin binding of β-carbolines (Figures 4 and 5). In the case of harmane, however, the poor ellipticity/absorbance ratios do not allow the reliable estimation of the HSA association constant; thus the influence of the FAs on the binding was investigated by a fluorescence spectroscopy method. Figure 7 shows the effect of palmitic acid on the emission spectrum of harmane in HSA solution. It can be observed that FA applied in equimolar concentration with HSA caused only a slight change; further addition, however, considerably enhanced the intensity of the peaks associated to the neutral form of harmane. Fluorescence titration of HSA with harmane in the presence of FA in 4-fold mole excess resulted in K_a value of 1.2 × 10^5 M^{-1} (Figure 7), which is about five times higher compared to that measured with FA-free HSA (Table 1). Similar results were obtained with myristic and oleic acid, but in the latter case, the maximal affinity increase was found at a [FA]:[HSA] ratio of 2.

The fluorescence quenching of the lone Trp214 residue is a reliable approach to establish the subdomain IIA binding of HSA ligands. Upon addition of norharmane and harmane (0–40 μM) to HSA solution (5 μM), no significant quenching could be detected (data not shown). The same result was obtained in the presence of palmitic acid, as well.

Molecular Docking Calculations. In view of the displacement results, the targeted docking procedure was performed placing the neutral form of norharmane into the pocket of subdomain IIIA to obtain the preferred binding orientation. This region consists of a modestly flexible, hydrophobic cavity

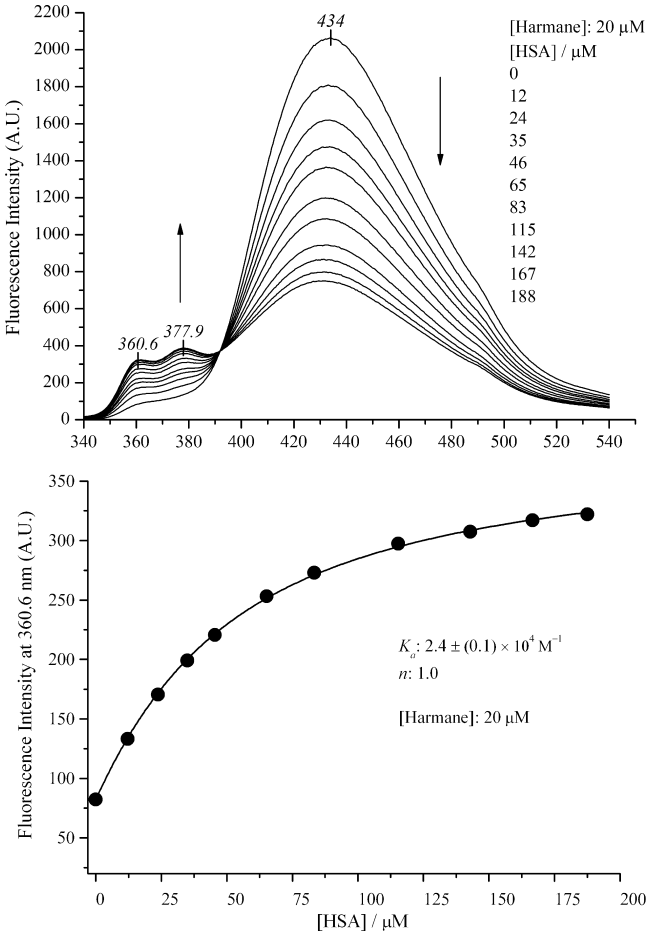

Figure 6. Top panel: Emission spectrum of harmane as a function of HSA concentration (2 mL of 20 μM harmane was titrated with aliquots of 500 μM HSA dissolved in the ligand solution). Bottom panel: Fluorescence intensities plotted against the HSA concentration of the sample solution. The solid line is the result of nonlinear fitting analysis.

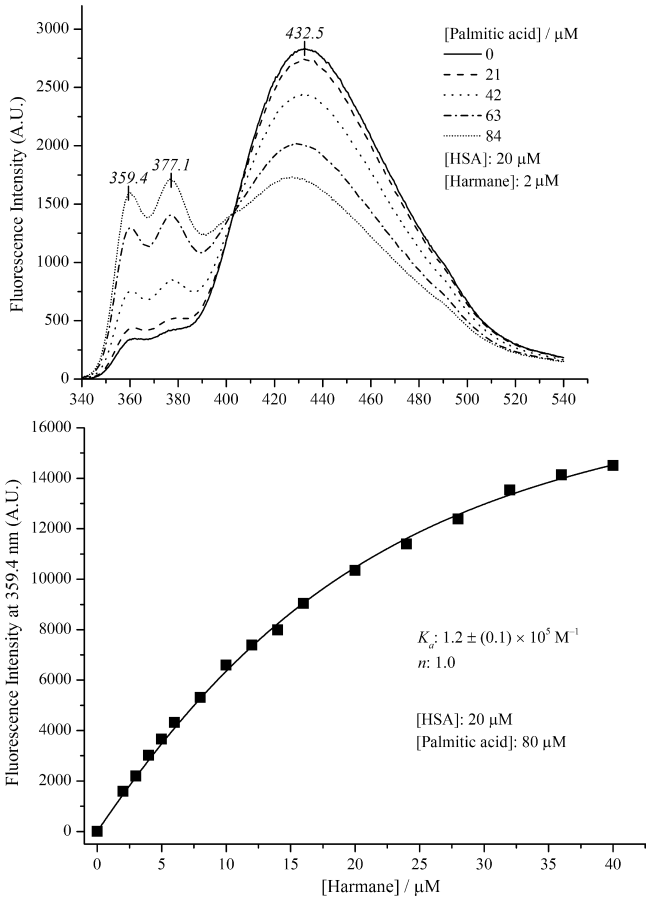

Figure 7. Effect of palmitic acid on the emission spectrum of harmane in HSA solution. Top panel: Emission spectra at different [FA]:[HSA] ratios. Bottom panel: Fluorescence intensities plotted against the harmane concentration of the sample solution containing 4:1 FA–HSA complexes. The solid line is the result of nonlinear fitting analysis.

and a polar side chain cluster (Arg410, Tyr411, Lys414, Ser489) near the pocket entrance.[7,9,26] That binding architecture accounts for the general preference of this site for aromatic compounds with a terminal acidic or electronegative group: the aromatic moiety of diflunisal, ibuprofen, indoxyl sulfate, iophenoxic, and dansylated amino acids occupies the same hydrophobic part of the pocket, while their electronegative groups are oriented in the vicinity of the polar patch where they form H-bonds with the Tyr411 side chain.[9,12,30] Since steric factors prevent the phenolic group of the general anesthetic propofol to interact with the polar cluster, the whole molecule is inserted deeply into the hydrophobic portion of the site.[31] In addition, site IIIA can simultaneously host two medium or long-chain FA molecules which bind cooperatively at the low- and high-affinity FA sites 3 and 4.[17,26,27] Distinctly from the FA ligands of the high-affinity site 4, the carboxylic head of FA bound to site 3 does not interact with the polar patch centered on Tyr411, but its methylene tail protrudes into the apolar subchamber where the aromatic rings of other site IIIA ligands are accommodated.

Molecular docking of the neutral form of norharmane was performed using the crystal structure of HSA complexed with myristic acids (PDB code 1BJ5).[26] Prior to the first docking procedure, only the site 3 FA molecule was removed from the complex. In that case, norharmane is buried within the hydrophobic pocket of the site (Figure 8), in a similar position to the aromatic moieties of ibuprofen, diflunisal, indoxyl sulfate, iophenoxic acid, and propofol.[9,12,31] The cavity wall is lined with apolar side chains (Ile388, Cys392, Leu407, Leu430, Val433, Cys438) suggesting the role of hydrophobic contacts that drive ligand binding here. Besides hydrophobic interactions, norharmane appeared capable of making a single H-bond between its −NH group and the carbonyl moiety of Leu430.

In the absence of both FA molecules, the docking results showed another potential binding location of norharmane in which the aromatic ring system is sandwiched between Tyr411 and Phe488 within 5 Å distance (Figure 8). Besides these $\pi-\pi$ stacking interactions, the pyrrole hydrogen forms a potential H-bond with the carbonyl oxygen of Phe488. Importantly, in this binding mode norharmane completely overlaps with the myristic acid molecule accommodated at the high-affinity FA site 4.

Harmane was also subjected to similar docking studies. In relation to norharmane, no relevant differences could be observed between their binding modes (data not shown).

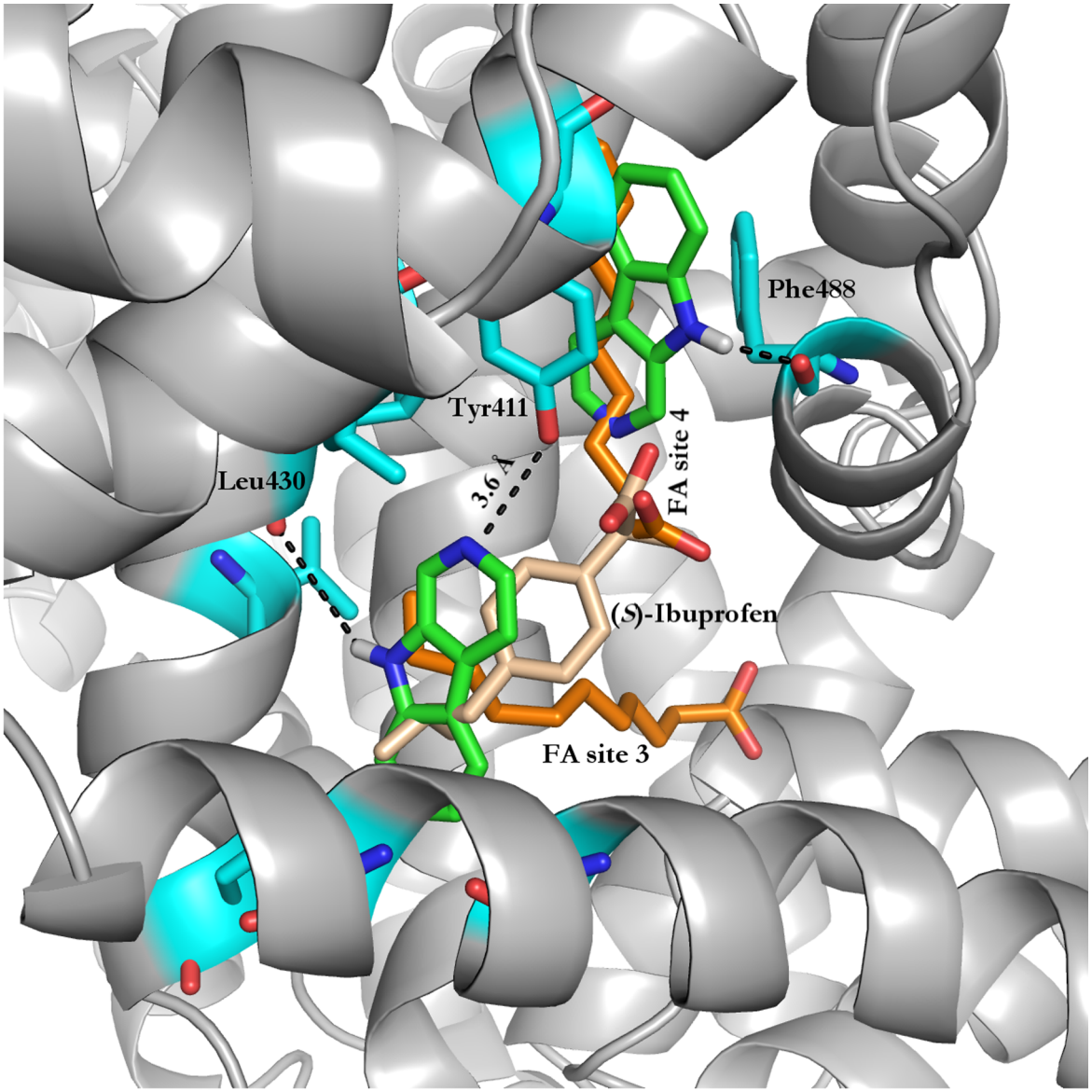

Figure 8. Two alternative binding positions of norharmane molecule docked into the subdomain IIIA cavity of HSA. FA (myristic acid) and ibuprofen ligands of the site are indicated. Dotted lines show intermolecular H-bonds.

DISCUSSION

Elucidation of the HSA Binding Site of Harmane and Norharmane. One of the fundamental issues to be clarified in the course of drug–HSA binding studies is the precise location of the binding site. Based on the finding that harmane and norharmane were found to increase the unbound concentration of L-tryptophan, Fenerty and Lindup suggested these compounds to be bound within subdomain IIIA.[15] These results showed much weaker binding of harmane in relation to norharmane. In concordance with this, our fluorescence studies indicated about a 7-fold affinity decrease of harmane. Domain I binding of norharmane has recently been proposed based on combined application of Förster resonance energy transfer (FRET), denaturation, and micropolarity studies.[14] Furthermore, taking into consideration fluorescence and phosphorescence data obtained with HSA and BSA, Gałęcki et al. have concluded that harmane is bound in the drug binding pocket of subdomain IIA.[16] Our data, however, do not support either the domain I or the subdomain IIA binding concept. Instead of displacement of the site IB specific CD marker biliverdin,[10] norharmane increased the ellipticity values of the bound pigment, suggesting that accommodation of norharmane occurs outside of domain I (Supporting Information, Figure 2). As it has previously been demonstrated, both site IIA and site IIIA ligands can allosterically modify the binding mode of biliverdin increasing its ICD amplitude.[10] Most likely, the same mechanism is responsible for the CD spectroscopic changes obtained with norharmane. Furthermore, in the presence of hemin which completely occupies the pocket in subdomain IB,[11] ICD activity of norharmane was preserved, indicating again that its binding site is located elsewhere on the protein. Subdomain IIA binding of β-carbolines can also be excluded since they could not quench the intrinsic fluorescence of HSA originated from the Trp214 residue situated near to the entrance of the site IIA pocket.

The selective site IIIA markers ibuprofen and naproxen were able to cancel the ICD peak of norharmane (Figure 3). Moreover, the ICD signal of carprofen which binds primarily at

dx.doi.org/10.1021/mp400531n | Mol. Pharmaceutics 2013, 10, 4706–4716

site IIIA[25] was completely brought to zero by norharmane, indicating a common binding region for these compounds. According to previous results, ibuprofen directly competes with carprofen and displaces it from site IIIA.[32] Noticeably, the close structural analogy between the aromatic moieties of carprofen and norharmane adds further support to their competitive HSA binding.

Origin and Nature of the HSA Binding Induced CD Activity of Norharmane. Despite the presence of a chiral center attached to the carbazole ring in carprofen, HSA binding induced CD pattern of this drug is similar to that measured with the achiral norharmane, suggesting the role of the asymmetric protein environment in generation of the ellipticity signals. Due to the completely planar and rigid aromatic ring system of norharmane and carprofen, these molecules could not acquire chiral conformation upon HSA binding.[33] Therefore, the ICD signals can be ascribed to nondegenerate chiral exciton coupling between their $\pi-\pi^*$ transitions and that of some adjacent aromatic residues of the binding site. Tryptophan and tyrosine side chains are the most important partners in such interactions since their intense $\pi-\pi^*$ bands are close to the UV bands of aromatic guest compounds.[34,35] Subdomain IIIA contains no tryptophan, but its Tyr411 residue is involved in H-bonding with various compounds bound here.[9,12,30,36] The spatial distance and orientation of the ligand molecule in relation to Tyr411 is defined by the stereochemistry of the binding locus and governs both the sign and the amplitude of the ICD bands.[35] As molecular docking calculations showed, norharmane is close to the phenolic ring of Tyr411 in both binding positions (≈5 Å) which is favorable for the intermolecular exciton coupling (Figure 8). It is to be noted, however, that "T"-shaped and parallel disposition of the interacting transition moments give rise to no ICD signal. Such a reason might be invoked to explain the lack of ICD activity of harmane bound to FA-free HSA. Presumably, due to steric interactions between the methyl group and binding site residues, the harmane molecule occupies a CD silent position.

Effects of Dietary FAs on the HSA Binding Properties of Harmane and Norharmane. In line with previous data, both UV absorption and fluorescence spectra indicated shifting of the cationic-neutral equilibrium of β-carbolines upon HSA binding in favor to the neutral species (Figures 1, 6, and 7). The protonation of the pyridine nitrogen is less favorable when ligands are accommodated in a hydrophobic binding environment. A comparison of the CD and absorption spectral features of harmane and norharmane obtained with fatted and defatted HSA samples reveals the dramatic effect of dietary FAs on the binding affinity as well as the binding mode of these alkaloids (Figures 2 and 5). Furthermore, the 2−3- and 5−10-fold increase of the association constants of norharmane and harmane, respectively, estimated from the CD and fluorescence titration data is the unequivocal indication of their much tighter binding within the resulting ternary complexes (Table 1). Additionally, inversion of the induced ellipticity bands of norharmane and generation of weak ICD activity of harmane provoked by the addition of FAs refer to the altered binding orientation of the molecules in relation to the adjacent aromatic residue. Theoretically, two alternative explanations can be offered for these changes. It can be assumed that norharmane possesses two classes of HSA binding sites, a primary and a secondary one which induces opposite CD signals. When FAs displace norharmane from its primary binding locus in subdomain IIIA, the alkaloid molecule is reassociated to the secondary site where it displayes inverted ICD signals. In such a case, however, the ICD profile should also be changed during the titration of FA-free HSA sample with norharmane. After saturation of the primary site, population of the secondary locus becomes more and more significant, and thus its opposite CD contribution should decrease and finally invert the positive ellipticity band of norharmane, as it has indeed been observed with diclofenac, the ICD spectrum of which displayes sign inversion above the 1:1 drug−HSA molar ratio.[37] Though our titration was terminated above 2 mol equivalents of norharmane, no such CD spectral changes were detected. Furthermore, if a secondary norharmane binding site would exist, then its contribution should also be manifested upon addition of ibuprofen and naproxen.[32] However, no CD sign inversion was seen during the titration of norharmane−HSA complexes with these drugs (Figure 3). In addition, these β-carbolines did not quench the fluorescence of fatted HSA which does not support their secondary, that is, site IIA binding. Taken together, these data suggest that the alkaloids remain bound within subdomain IIIA even in the presence of FAs which allosterically enhance their binding affinity and invert the ICD spectrum. Such kinds of positive allosteric binding interactions between β-carboline alkaloids and nonesterified FAs may have a strong impact on the biologically active, free plasma level of these agents. For instance, upon FA binding induced affinity increase, the free fraction of harmane drops from 7 to <1% (Table 1). Myristic and palmitic acid enhance the HSA association of β-carbolines at a 4:1 FA−HSA ratio, but oleic acid added in two or three mole equivalents produces a similar effect. Between 0.1 and 2 mol of FA are bound to HSA under physiological conditions, but this ratio can rise to 6:1 in pathological states such as obesity, diabetes, liver, and cardiovascular diseases. Accordingly, the free plasma fraction of harmane and norharmane can fluctuate both in normal and pathological conditions depending on the particular FA binding profile of HSA.

Molecular Docking of Norharmane to Site IIIA. Docking calculations suggested two possible binding locations of norharmane inside the IIIA pocket. The molecule can be accommodated at the entrance of the hydrophobic tunnel of FA site 4, where it is stabilized by $\pi-\pi$ stacking (Tyr411, Phe488) and H-bonding interactions (Figure 8). It is worth mentioning that, according to NMR data, the nitrobenzene moiety of a Bcl-2 family inhibitor anticancer agent occupies the same region and it is stacked upon Tyr411.[38] In this binding position the pyridine ring of norharmane sterically clashes with the carboxylic group of ibuprofen, which explains the displacement effect obtained by using this drug. A similar assumption can be raised in relation to binding competitions found with naproxen and carprofen. In line with this picture, propofol which does not interact with Tyr411[31] exhibited very weak competition against norharmane (Figure 3). Upon occupation of the high-affinity FA site 4 by its lipid ligand, norharmane is translocated into the fully apolar subpocket where aromatic rings of typical site IIIA ligands are also accommodated.[9,12,30] In this novel binding position the molecule establishes several van der Waals contacts with the adjacent apolar residues and forms a single H-bond to the carbonyl oxygen of Leu430. Importantly, as crystallographic analyses have revealed this carbonyl group makes H-bonding with various site IIIA ligands including propofol, halothane, and indoxyl sulfate.[9,31] Furthermore, the occupation of the FA site 3 may contribute to the higher-affinity binding of β-carbolines by

allowing cooperative interactions between them and the methylene tail of the site 3 FA molecule. Curiously, in contrast to the other drug ligands of site IIIA, FAs do not displace either harmane or norharmane but cobind with them within the pocket. Distinctly from the acidic compounds like ibuprofen, indoxyl sulfate, and iophenoxic acid, β-carbolines lack electronegative substituent thus their binding is not impacted by formation of H-bond with Tyr411. In addition, their relatively small size and completely flat shape might allow greater freedom to access more subsites and thus to bind together with FAs without steric interference.

CONCLUSIONS

Our work reveals that allostery is a prominent regulatory mechanism in the HSA binding of harmane and norharmane. The binding location of these basic molecules was successfully mapped by displacement experiment and assigned to subdomain IIIA which harbors two FA sites as well. The peculiar CD, absorption, and fluorescence spectroscopic changes observed upon addition of FAs to β-carboline−HSA complexes refer to their cooperative accommodation within the subdomain IIIA pocket. This unique, intradomain FA−alkaloid allosteric binding interaction accounts for the increase of the affinity constants, for inversion of the ICD bands, for generation of CD activity of harmane, and for enhanced fluorescence emission of the neutral form of the ligands. The results also imply that, depending on the number and chemical constitution of FAs bound to HSA, the pharmacologically active free plasma level of these β-carboline alkaloids may fluctuate both under normal as well as pathological conditions.

ASSOCIATED CONTENT

Supporting Information

Norharmane-HSA CD titration data measured in the absence and in the presence of myristic acid and CD/absorption spectral changes of HSA bound biliverdin recorded upon addition of norharmane. This material is available free of charge via the Internet at http://pubs.acs.org.

AUTHOR INFORMATION

Corresponding Author

*E-mail: zsila.ferenc@ttk.mta.hu. Fax: (+36) 1-438-1145.

Notes

The authors declare no competing financial interest.

ACKNOWLEDGMENTS

The generosity of some colleagues by supplying (±)-carprofen (Dr. László Gagyi, S.C. VIM SPECTRUM S.R.L., Romania) and harmane samples (Dr. András Kotschy, Servier Research Institute of Medicinal Chemistry, Budapest, Hungary) is highly acknowledged.

ABBREVIATIONS

CD, circular dichroism; FA, fatty acid; HSA, human serum albumin; NH, norharmane

REFERENCES

(1) Cao, R.; Peng, W.; Wang, Z.; Xu, A. β-Carboline alkaloids: biochemical and pharmacological functions. *Curr. Med. Chem.* **2007**, *14*, 479−500.

(2) Pfau, W.; Skog, K. Exposure to β-carbolines norharman and harman. *J. Chromatogr., B* **2004**, *802*, 115−126.

(3) Rommelspacher, H.; May, T.; Susilo, R. β-Carbolines and tetrahydroisoquinolines: Detection and function in mammals. *Planta Med.* **1991**, *57*, S85−92.

(4) Anderson, N. J.; Tyacke, R. J.; Husbands, S. M.; Nutt, D. J.; Hudson, A. L.; Robinson, E. S. In vitro and ex vivo distribution of [^{3}H]harmane, an endogenous β-carboline, in rat brain. *Neuropharmacology* **2006**, *50*, 269−276.

(5) Haghdoost-Yazdi, H.; Hosseini, S. S.; Faraji, A.; Nahid, D.; Jahanihashemi, H. Long term exposure to norharman exacerbates 6-hydroxydopamine-induced parkinsonism: possible involvement of L-type Ca^{2+} channels. *Behav. Brain Res.* **2010**, *215*, 136−140.

(6) Fanali, G.; di Masi, A.; Trezza, V.; Marino, M.; Fasano, M.; Ascenzi, P. Human serum albumin: From bench to bedside. *Mol. Aspects Med.* **2012**, *33*, 209−290.

(7) Curry, S. Lessons from the crystallographic analysis of small molecule binding to human serum albumin. *Drug Metab. Pharmacokinet.* **2009**, *24*, 342−357.

(8) Varshney, A.; Sen, P.; Ahmad, E.; Rehan, M.; Subbarao, N.; Khan, R. H. Ligand binding strategies of human serum albumin: how can the cargo be utilized? *Chirality* **2010**, *22*, 77−87.

(9) Ghuman, J.; Zunszain, P. A.; Petitpas, I.; Bhattacharya, A. A.; Otagiri, M.; Curry, S. Structural basis of the drug-binding specificity of human serum albumin. *J. Mol. Biol.* **2005**, *353*, 38−52.

(10) Zsila, F. Subdomain IB is the third major drug binding region of human serum albumin: Toward the three-sites model. *Mol. Pharmacol.* **2013**, *10*, 1668−1682.

(11) Zunszain, P. A.; Ghuman, J.; Komatsu, T.; Tsuchida, E.; Curry, S. Crystal structural analysis of human serum albumin complexed with hemin and fatty acid. *BMC Struct. Biol.* **2003**, *3*, 6.

(12) Ryan, A. J.; Chung, C. W.; Curry, S. Crystallographic analysis reveals the structural basis of the high-affinity binding of iophenoxic acid to human serum albumin. *BMC Struct. Biol.* **2011**, *11*, 18.

(13) Fitos, I.; Visy, J.; Simonyi, M. Binding of vinca alkaloid analogues to human serum albumin and to α_1-acid glycoprotein. *Biochem. Pharmacol.* **1991**, *41*, 377−383.

(14) Chakrabarty, A.; Mallick, A.; Haldar, B.; Das, P.; Chattopadhyay, N. Binding interaction of a biological photosensitizer with serum albumins: a biophysical study. *Biomacromolecules* **2007**, *8*, 920−927.

(15) Fenerty, C. A.; Lindup, W. E. Effect of β-carboline derivatives on the binding of L-tryptophan and diazepam to bovine and human albumin. *Biochem. Pharmacol.* **1991**, *41*, 1589−1594.

(16) Gałęcki, K.; Despotović, B.; Galloway, C.; Ioannidis, A. G.; Janani, T.; Nakamura, Y.; Oluyinka, G. Binding of harmane to human and bovine serum albumin: fluorescence and phosphorescence study. *Biotechnol. Food Sci.* **2012**, *76*, 3−12.

(17) Curry, S. Plasma albumin as a fatty acid carrier. *Adv. Mol. Cell Biol.* **2004**, *33*, 29−46.

(18) Zsila, F.; Bikádi, Z.; Simonyi, M. Probing the binding of the flavonoid, quercetin to human serum albumin by circular dichroism, electronic absorption spectroscopy and molecular modelling methods. *Biochem. Pharmacol.* **2003**, *65*, 447−456.

(19) Breustedt, D. A.; Schonfeld, D. L.; Skerra, A. Comparative ligand-binding analysis of ten human lipocalins. *Biochim. Biophys. Acta* **2006**, *1764*, 161−173.

(20) Bikadi, Z.; Hazai, E. Application of the PM6 semi-empirical method to modeling proteins enhances docking accuracy of AutoDock. *J. Cheminform.* **2009**, *1*, 15.

(21) Tarzi, O. I.; Erra-Balsells, R. Effect of chlorine as substituent on the photochemistry and acid-base properties of β-carboline alkaloids. *J. Photochem. Photobiol., B* **2006**, *82*, 79−93.

(22) Mallick, A.; Das, P.; Chattopadhyay, N. Photophysics of norharmane in solution phase: From homogeneous to micro-heterogeneous environments. *J. Photochem. Photobiol., C* **2010**, *11*, 62−72.

(23) Fehske, K. J.; Jahnchen, E.; Muller, W. E.; Stillbauer, A. Azapropazone binding to human serum albumin. *Naunyn Schmiedebergs Arch. Pharmacol.* **1980**, *313*, 159−163.

(24) Bertucci, C.; Andrisano, V.; Gotti, R.; Cavrini, V. Use of an immobilised human serum albumin HPLC column as a probe of drug-

protein interactions: the reversible binding of valproate. *J. Chromatogr., B* **2002**, *768*, 147−155.
(25) Rahman, M. H.; Maruyama, T.; Okada, T.; Yamasaki, K.; Otagiri, M. Study of interaction of carprofen and its enantiomers with human serum albumin I. Mechanism of binding studied by dialysis and spectroscopic methods. *Biochem. Pharmacol.* **1993**, *46*, 1721−1731.
(26) Bhattacharya, A. A.; Grune, T.; Curry, S. Crystallographic analysis reveals common modes of binding of medium and long-chain fatty acids to human serum albumin. *J. Mol. Biol.* **2000**, *303*, 721−732.
(27) Simard, J. R.; Zunszain, P. A.; Hamilton, J. A.; Curry, S. Location of high and low affinity fatty acid binding sites on human serum albumin revealed by NMR drug-competition analysis. *J. Mol. Biol.* **2006**, *361*, 336−351.
(28) Fujiwara, S.; Amisaki, T. Steric and allosteric effects of fatty acids on the binding of warfarin to human serum albumin revealed by molecular dynamics and free energy calculations. *Chem. Pharm. Bull.* **2011**, *59*, 860−867.
(29) Chuang, V. T.; Otagiri, M. How do fatty acids cause allosteric binding of drugs to human serum albumin? *Pharm. Res.* **2002**, *19*, 1458−1464.
(30) Ryan, A. J.; Ghuman, J.; Zunszain, P. A.; Chung, C. W.; Curry, S. Structural basis of binding of fluorescent, site-specific dansylated amino acids to human serum albumin. *J. Struct. Biol.* **2011**, *174*, 84−91.
(31) Bhattacharya, A. A.; Curry, S.; Franks, N. P. Binding of the general anesthetics propofol and halothane to human serum albumin. High resolution crystal structures. *J. Biol. Chem.* **2000**, *275*, 38731−38738.
(32) Rahman, M. H.; Maruyama, T.; Okada, T.; Imai, T.; Otagiri, M. Study of interaction of carprofen and its enantiomers with human serum albumin II. Stereoselective site-to-site displacement of carprofen by ibuprofen. *Biochem. Pharmacol.* **1993**, *46*, 1733−1740.
(33) Zsila, F.; Bikadi, Z.; Simonyi, M. Unique, pH-dependent biphasic band shape of the visible circular dichroism of curcumin-serum albumin complex. *Biochem. Biophys. Res. Commun.* **2003**, *301*, 776−782.
(34) Zsila, F. Aromatic side-chain cluster of biotin binding site of avidin allows circular dichroism spectroscopic investigation of its ligand binding properties. *J. Mol. Recognit.* **2011**, *24*, 995−1006.
(35) Zsila, F.; Iwao, Y. The drug binding site of human α_1-acid glycoprotein: insight from induced circular dichroism and electronic absorption spectra. *Biochim. Biophys. Acta* **2007**, *1770*, 797−809.
(36) Petitpas, I.; Petersen, C. E.; Ha, C. E.; Bhattacharya, A. A.; Zunszain, P. A.; Ghuman, J.; Bhagavan, N. V.; Curry, S. Structural basis of albumin-thyroxine interactions and familial dysalbuminemic hyperthyroxinemia. *Proc. Natl. Acad. Sci. U.S.A.* **2003**, *100*, 6440−6445.
(37) Yamasaki, K.; Rahman, M. H.; Tsutsumi, Y.; Maruyama, T.; Ahmed, S.; Kragh-Hansen, U.; Otagiri, M. Circular dichroism simulation shows a site-II-to-site-I displacement of human serum albumin-bound diclofenac by ibuprofen. *AAPS PharmSciTech* **2000**, *1*, E12.
(38) Oltersdorf, T.; Elmore, S. W.; Shoemaker, A. R.; Armstrong, R. C.; Augeri, D. J.; Belli, B. A.; Bruncko, M.; Deckwerth, T. L.; Dinges, J.; Hajduk, P. J.; Joseph, M. K.; Kitada, S.; Korsmeyer, S. J.; Kunzer, A. R.; Letai, A.; Li, C.; Mitten, M. J.; Nettesheim, D. G.; Ng, S.; Nimmer, P. M.; O'Connor, J. M.; Oleksijew, A.; Petros, A. M.; Reed, J. C.; Shen, W.; Tahir, S. K.; Thompson, C. B.; Tomaselli, K. J.; Wang, B.; Wendt, M. D.; Zhang, H.; Fesik, S. W.; Rosenberg, S. H. An inhibitor of Bcl-2 family proteins induces regression of solid tumours. *Nature* **2005**, *435*, 677−681.